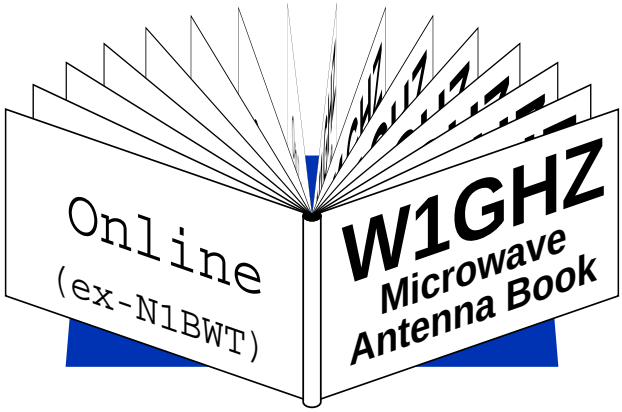

Appendix 6C
Electromagnetic Fields in Feed Antennas

Paul Wade W1GHZ ©2001

Calculated near-fields

One of the benefits of using a 3D simulator to calculate antenna patterns is that we are able to calculate the electromagnetic fields in the near-field, inside and close to the antenna, as well as the far-field radiation patterns. The diagrams included here and for some of the feed antennas in Chapter 6 were generated by the Zeland[1] **Fidelity** software. The **NEC2** software used for calculation of many of the feeds calculates currents on the segments of the antenna model, but only in tabular form, not amenable to visual interpretation. Examination of the near-field plots for these feed antennas may provide some insight into the operation of the feeds and perhaps aid in the development of new designs.

In other sections of this chapter, near-field plots are shown for some of the feeds, but more explanation may be necessary to understand them. The intent of this appendix is to use the diagrams as a visual aid to intuition of the feed operation, not as a rigorous explanation. Any rigorous explanation of field theory inevitably requires serious mathematics. If you are inclined to tackle it, I recommend George Southworth's venerable *Principles and Applications of Waveguide Transmission*[2]. He develops the field theory directly from Maxwell's equations in a clear, step-by-step, manner, without pretending that the math is obvious or leaving the difficult parts "as an exercise for the student." Another, more concise, explanation by Jull[3] reveals the secret that other books hide with tensor notation: if we are solving Maxwell's equations for plane waves, then the partial derivatives may be replace by $j\omega$, so that numerical computation is practical.

Until very recently, field diagrams like this were only available for very simple geometries for which hand calculation and sketching was feasible, like the field line drawings[4] of waveguide modes from section 6.5 — some of them are shown in Figure 6C-1. The only other alternative was to build a model for a frequency low enough that the fields could be tediously probed and measured in fine detail. The availability of very powerful personal computers and advances in software has made computations like these possible even for amateur use.

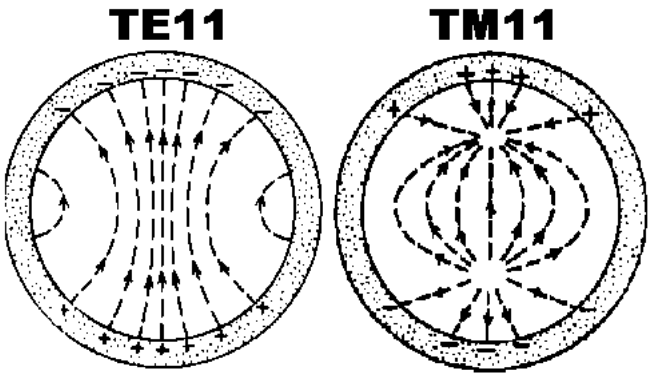

Figure 6C-1

Open waveguides

Some of the simplest feed antennas are plain open-ended waveguides. They have the additional advantage that simple waveguides are described in detail in a number of books, so we can verify that what we see in the near-field diagrams corresponds to the published fields which were derived mathematically.

Our first example is an open-ended section of WR-90 waveguide, commonly used at 10 GHz. The main area of interest is the electric field at the aperture, since this has the largest influence on the far-field radiation pattern. Since the aperture is the open end of a waveguide, we could expect the electric field at the aperture to be similar to the field inside the waveguide. The electric field in a rectangular waveguide is well-known[2]; it is uniform in the narrow direction, or E-plane, while in the wide direction (H-plane) it is described by $\cos(\pi x/a)$, where a is the wide dimension and x is the distance from the center of the guide, so that the field intensity is maximum in the center and falls off sinusoidally to zero at the side wall. Figure 6C-2 is a graphical depiction of the cosine field distribution inside the guide.

Figure 6C-2

The far-field pattern of an antenna and the near-field distribution in the aperture plane are a spatial Fourier Transform pair, in the same way that a time-domain waveform has an associated spectrum in the frequency domain, related to each other by a Fourier Transform. We will not tackle the subject in any depth, but there are a couple of basic properties of Fourier Transform pairs we should be aware of:

1. Increasing the spectrum width in one half of a transform pair decreases the width of the spectrum in the other half of the pair. Thus, an antenna with a small aperture will have a broader far-field beamwidth than an antenna with a larger aperture. An infinitely small aperture, or point source, radiates uniformly in all directions. Sidelobe spacing is also inversely proportional to aperture size.
2. Abrupt changes in a spectrum will transform to a broader spectrum in the other half of the transform pair. This means that an antenna with a smoothly tapered aperture distribution will have smaller sidelobes in the far-field pattern.

For the simple field distributions found inside rectangular waveguide, the Fourier Transforms are simple and may be looked up in reference books[5]. The uniform rectangular distribution in the E-plane transforms to a *sin(x)/x* pattern, one with large distinct sidelobes, somewhat like Figure 1-1, since the field changes abruptly at the waveguide boundary. The cosine distribution in the H-plane transforms to a cosine pattern in the far-field, like Figure 4-4, but with additional small sidelobes because the idealized cosine field does not extend beyond the waveguide boundary – a smaller abrupt change. Thus, we could easily sketch an idealized far-field pattern for the open-ended rectangular waveguide, if the aperture fields were the same as those inside the guide.

However, the real aperture fields from an open-ended waveguide are not neatly contained within the guide. Figure 6C-3 shows the calculated electric fields, or E-fields, in and around the waveguide using a color map, with red indicating the maximum field intensity and each color step on the color bar showing 5 dB lower intensity than the box above it. The units for electric field intensity are Volts/Meter.

The aperture diagrams in the center show the same distribution within the waveguide as Figure 6C-2; the upper one, marked "*close up, 3.5 dB/box*" has a finer intensity scale to better show this pattern. The uniform electric field in the narrow direction means that there is high field intensity along the long wall of the rim at the aperture. The areas of high field intensity along the wall generate currents in the long wall rim of the guide at the aperture. These currents behave as additional radiation sources, radiating to the sides and rear; these interfere with the desired radiation source in the center of the guide, resulting in undesired radiation to the sides and rear. Figure 1-2e is an illustration of the radiation resulting from two sources of radiation; the open waveguide, with three unequal sources, is more complex.

Figure 6C-3 also includes two cross sections through the center of the waveguide. On the left is a section along the E-plane, including the probe where the waveguide is excited from a coaxial source. On the right is a section along the H-plane, showing the wide dimension of the rectangular waveguide.

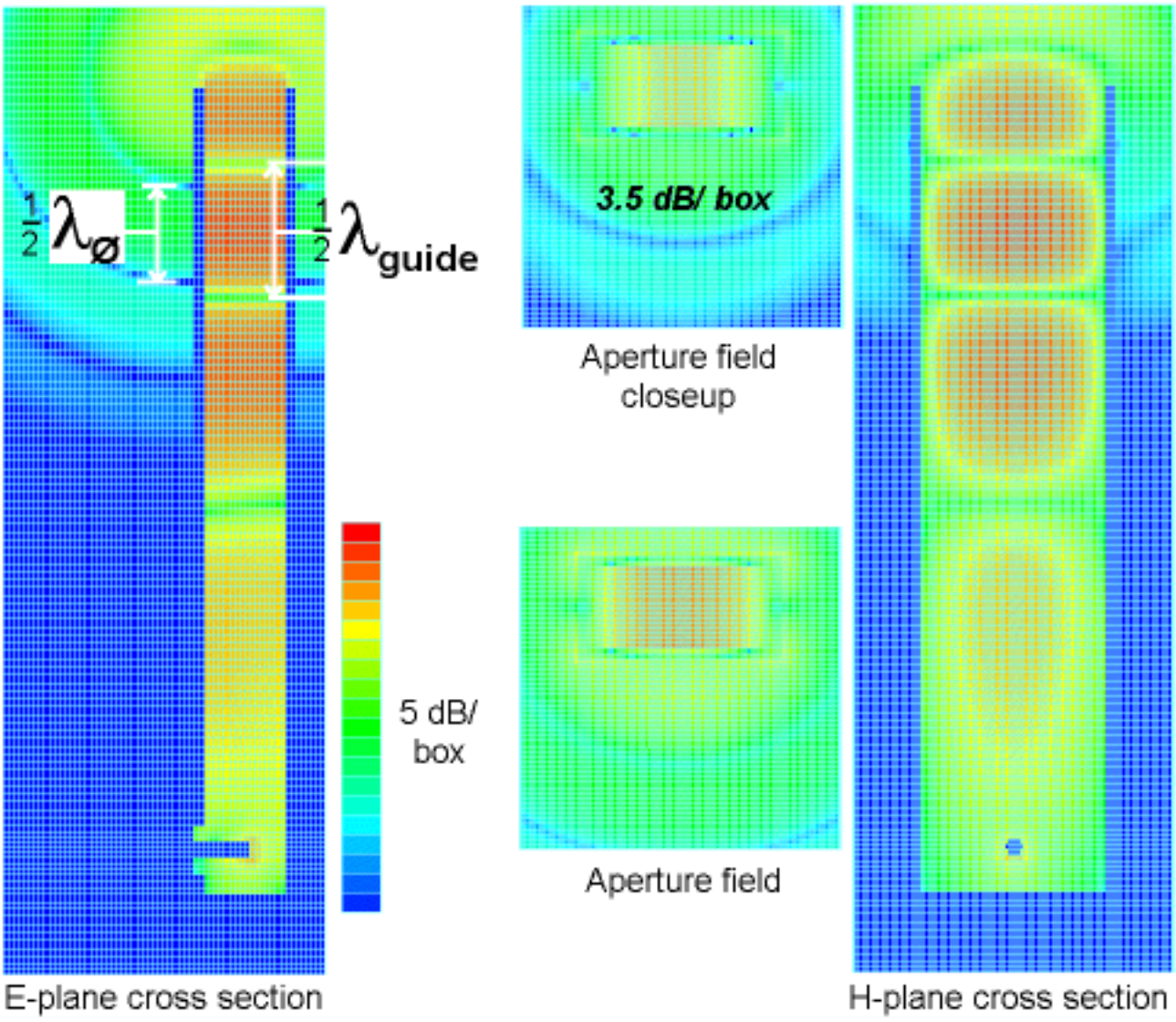

Figure 6C-3 Electric Fields in open WR-90 waveguide feed
by Zeland Fidelity

In the center of the figure is a section along the plane of the aperture, at the open end of the waveguide. If we could see into the waveguide past the aperture, the probe would be vertical, starting at the bottom of the waveguide, so that we are seeing the aperture in vertical polarization. This polarization view, with the E-field vertically polarized, seems to be the standard orientation for field and pattern computations, including **NEC2**. If you must see horizontal polarization, rotate the page or tilt your head in front of your monitor.

All of the near-field diagrams in this book have the same standard orientation as Figure 6C-3.

Once we have established the orientation, we can further examine the behavior of the fields. The waveguide is excited by the probe, and energy propagates upward in both the right and left diagrams. When it reaches the open end at the top, it radiates out into space: mainly in the forward direction, but some energy is radiated to the sides and rear due to the currents in the long wall rim. We can see in Figure 6C-4 that the actual radiation pattern of an open rectangular waveguide has significant side and rear lobes, but the additional radiation from the rim smears them together so it is difficult to discern distinct lobes.

As the energy propagates along the waveguide from the bottom, we see areas of high intensity separated by low intensity — we have captured the electric field at an instant of time, and are looking at the sinusoidal voltage maxima and minima. The distance between two minima is a half-wavelength. Note that the wavelength inside the waveguide, or guide wavelength, is *longer* than the waveguide on the outside, in free space; these wavelengths are marked in the left-hand diagram.

We are not restricted to a static view at one time. We may capture a series of instantaneous field views show showing a pulse propagating in an antenna and into space, and assemble these into a short animation showing the field in motion. Appendix 6D includes video clips animating all the feeds described here, as well as several others.

Near the probe, the minima and maxima are less clear — we may interpret this as higher-order *evanescent* waveguide modes, with different wavelengths, being excited by the probe but only propagating a short distance since their wavelengths are beyond cutoff in this waveguide. For good antenna performance, the waveguide should be long enough to eliminate any unwanted modes so that only the dominant mode reaches the aperture; one guide wavelength is usually considered adequate.

WR-90 open waveguide at 10.368 GHz, by Zeland Fidelity

Figure 6C-4

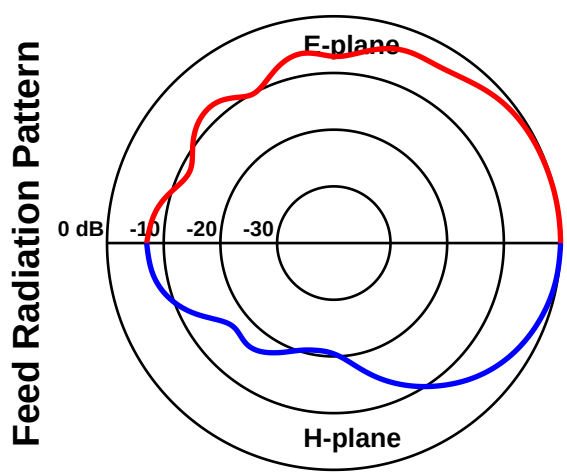

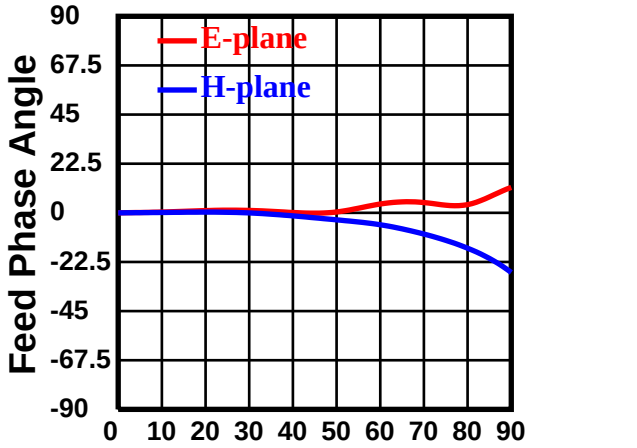

Dish diameter = 10 λ Feed diameter = 1 λ

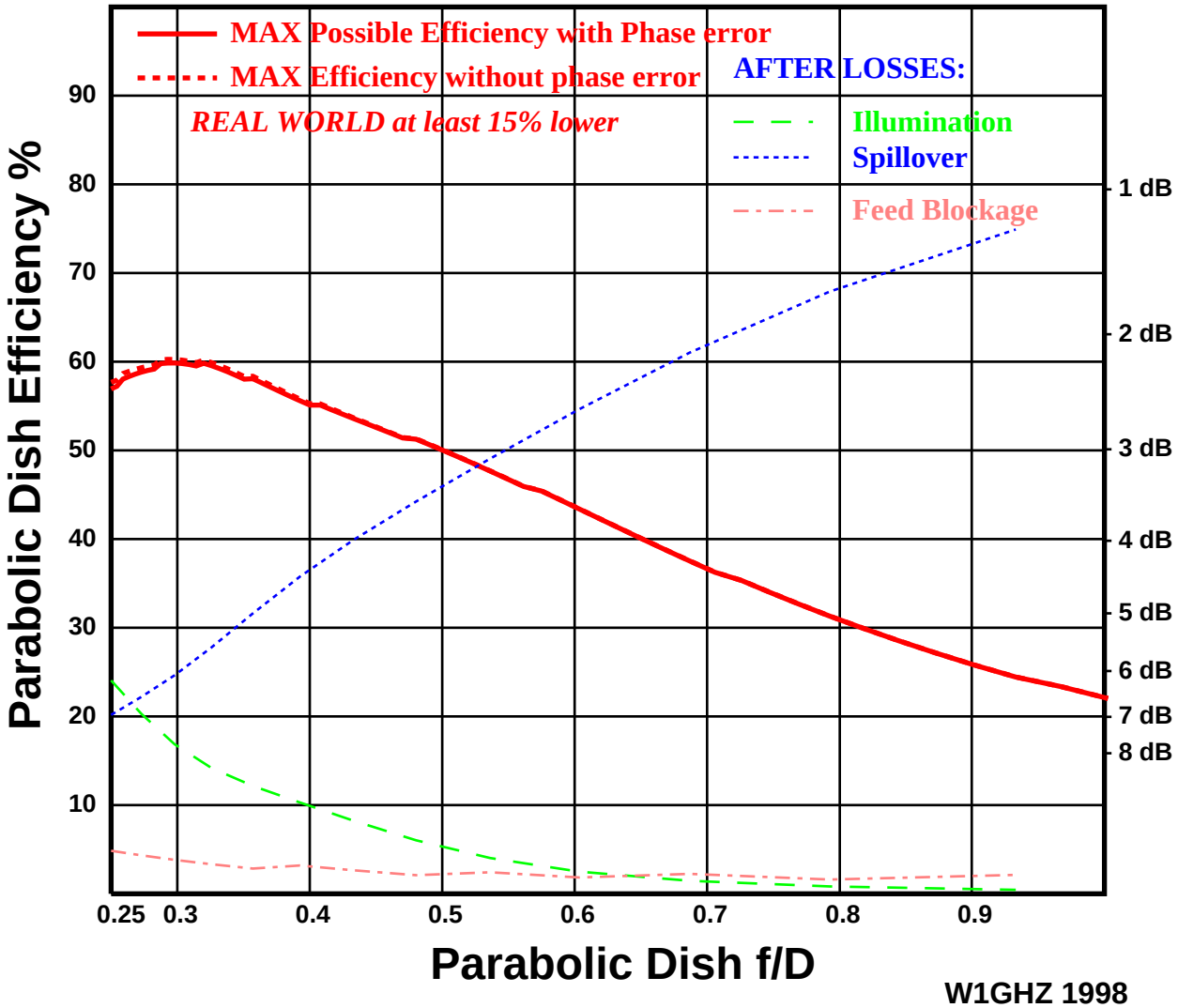

W1GHZ 1998

The electric field of an open-ended circular waveguide, shown in Figure 6C-5, is very similar to the open rectangular waveguide. However, the aperture field is more complex, requiring Bessel functions for a mathematical description; Southworth[2] skips ahead to diagrams like Figure 6C-1, and we shall also resort to pictures. Like the rectangular guide, the aperture field intensity for the dominant mode is fairly uniform in the H-plane and has a maximum at the center in the E-plane, but the maximum region has a constricted waist in the center, as seen in Figure 6C-5. Compare this with Figure 6C-1, which depicts the electric field as a series of lines, with closer spacing indicating higher field intensity. Also like the rectangular guide, there is high field intensity at the guide walls at the top and bottom of the aperture; the one at the top of the aperture field plot is quite evident. The resultant far-field radiation pattern has the large side and rear lobes as we saw in Figure 6.3-1.

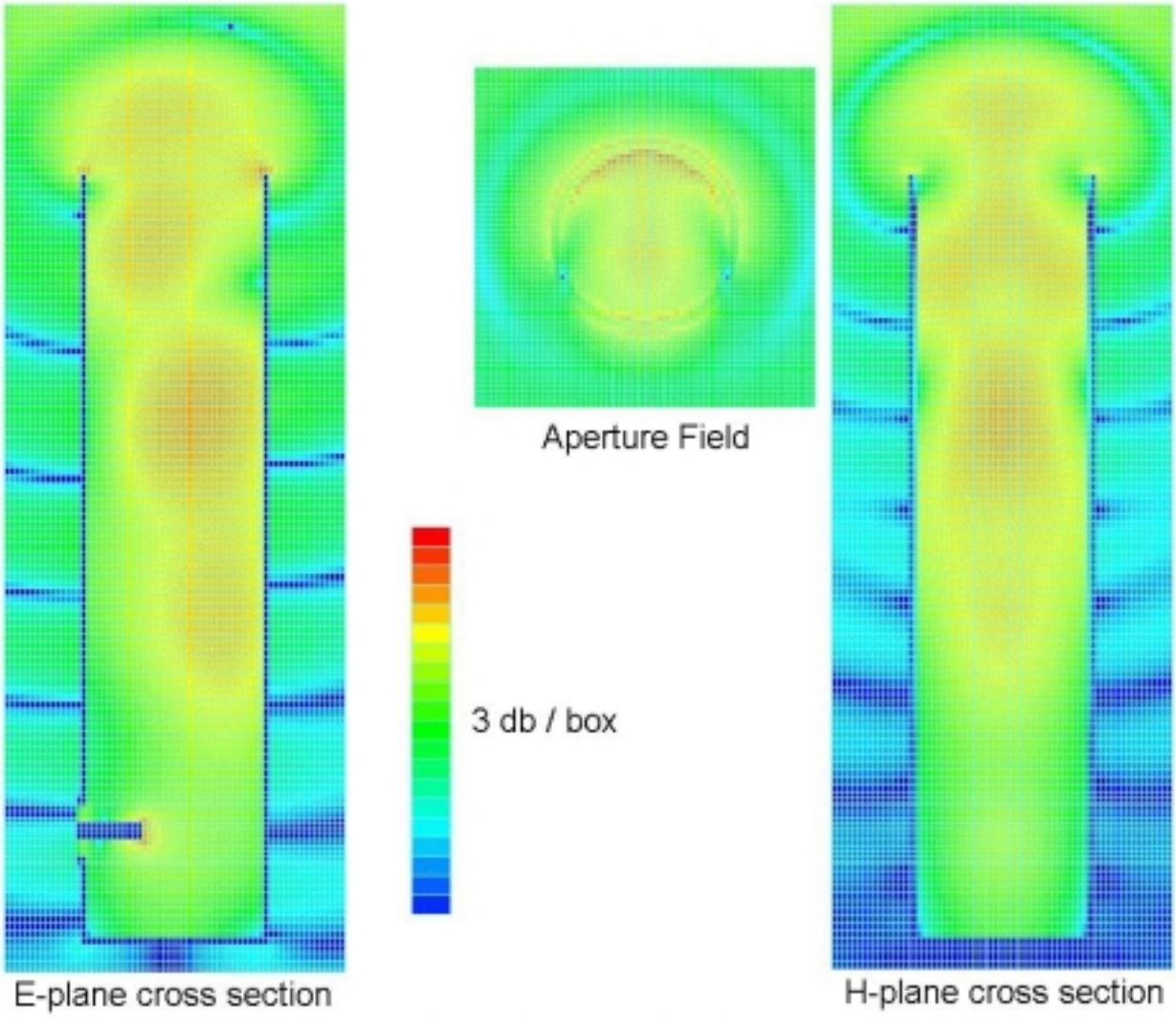

Figure 6C-5 Electric Fields in open circular waveguide feed
by Zeland Fidelity

Magnetic fields

Any electromagnetic wave has both an electric field, or E-field, and an orthogonal magnetic field, or H-field. The electric field is more useful for our purpose: visualization and intuition. In many cases, the magnetic field might be more confusing than illuminating. In any case, I only saved the magnetic field for one example, a dual-band feed for 10 and 24 GHz by W5ZN[6] described in Section 6.9. At 10 GHz, this feed behaves just like an open-ended circular waveguide – the 24 GHz waveguide section at the back is well beyond cutoff so it has essentially no effect at 10 GHz.

Figure 6C-6 shows both the electric fields and magnetic fields for this feed; the magnetic field plots are below the electric. Decide for yourself whether the magnetic fields offer any additional insight.

Power flowing in a waveguide is the vector cross-product of the electric and magnetic fields, with both magnitude and direction:

$$\mathbf{P} = \mathbf{E} \times \mathbf{H}$$

Since our color diagrams only show magnitude of the fields, they are of little use for the vector calculation. We can see that both electric and magnetic fields are strong in the aperture, so power is flowing, but we cannot discern the direction.

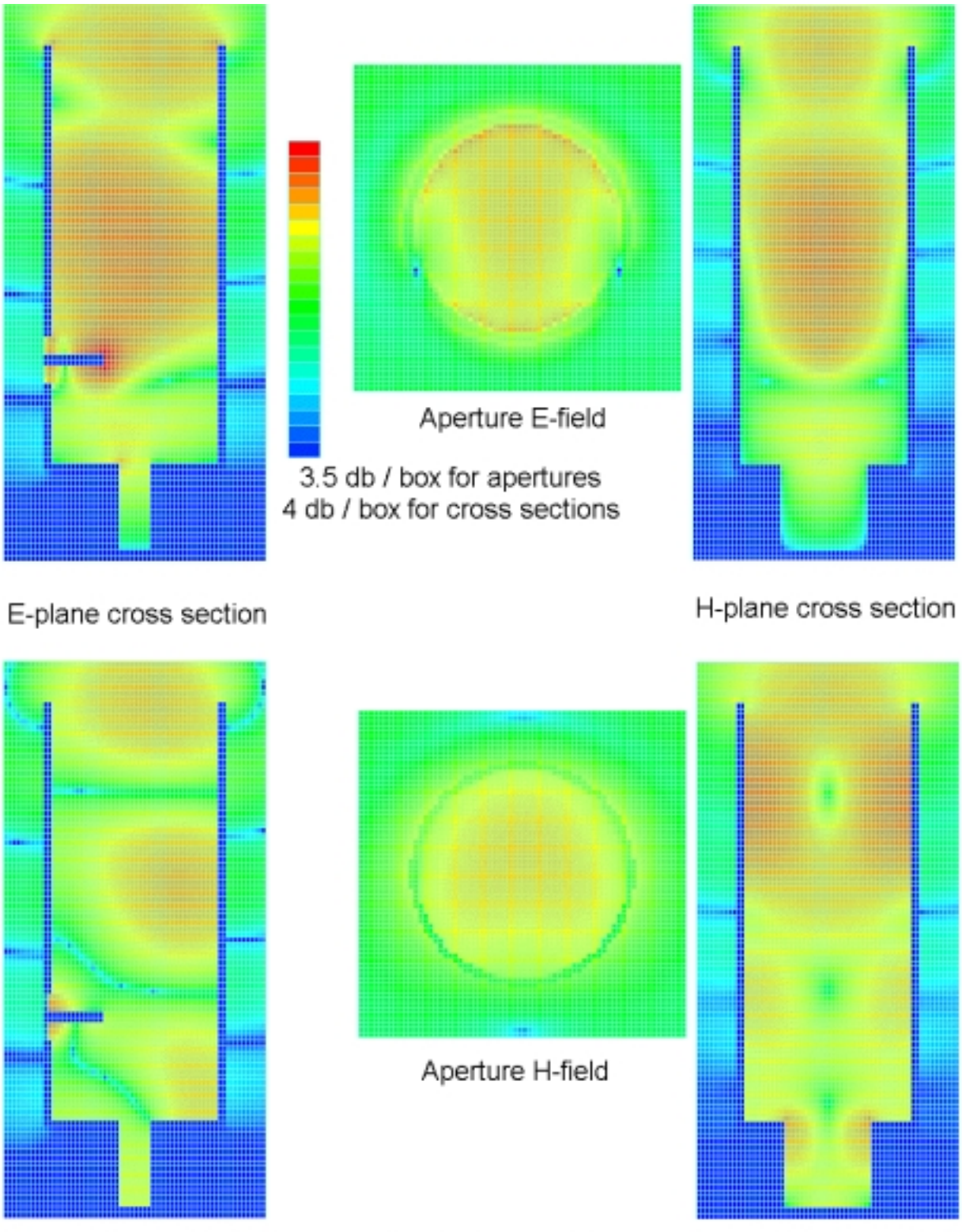

Figure 6C-6 Feed with both E- and H- Fields

by Zeland Fidelity

Sidelobe reduction in circular feeds

One of the primary objectives in feed antenna design is to maximize the radiation from the feed that illuminates the reflector. Clearly, radiation to the sides and rear does not reach the reflector and should be minimized. W2IMU[7] stated that the goal of his dual-mode feed was to "cancel the electric field at the aperture boundary," — the high fields we see around the aperture in Figure 6C-5. Figure 6C-7 shows the electric field in the W2IMU dual-mode feed. The second mode, excited by the flare to the larger diameter, is not clearly evident in the diagram, but the improvement in the aperture field is obvious. The field intensity is maximum in the center of the aperture and much less at the rim, or boundary, in all directions, with reduced field intensity along the outside of the guide walls. The end result is the low sidelobe levels seen in Figure 6.5-1.

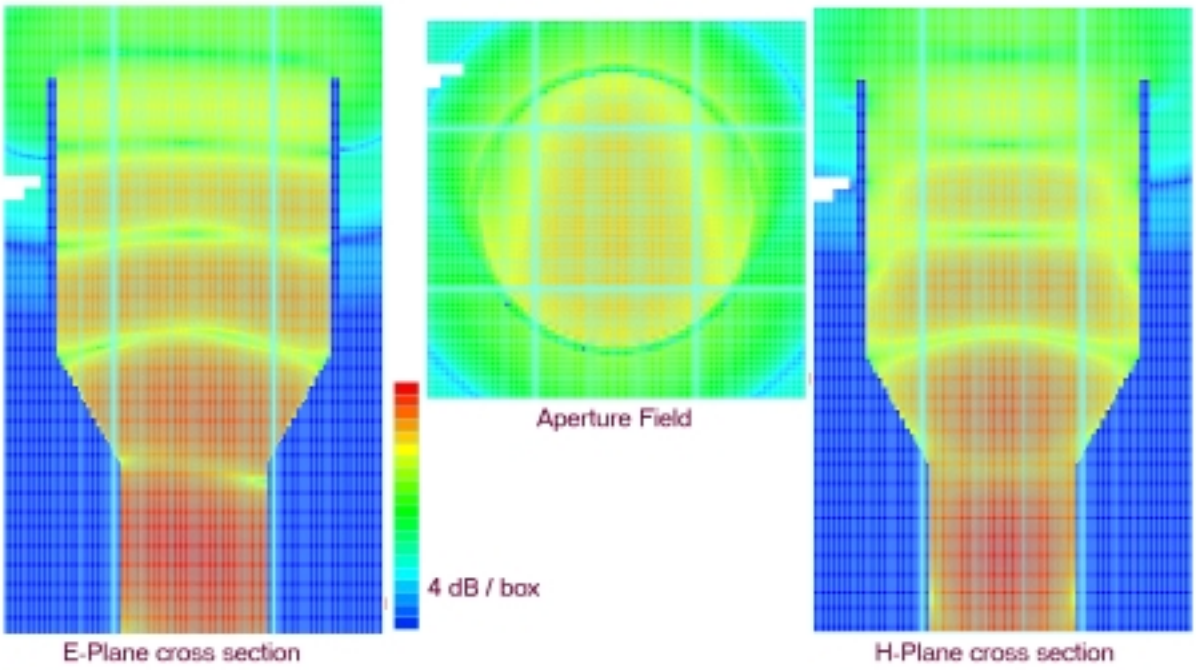

Figure 6C-7 Electric Fields in W2IMU dual-mode feedhorn
by Zeland Fidelity

However, the second mode is clearly obvious in another version of the dual-mode feed — the bad imitation of the W2IMU feed we saw in section 6.5. The bad imitation, an unmodified plumbing fitting, has a flare angle more abrupt than calculated for the change in diameters. The result is that an excessively large second mode is excited and dominates the aperture field in Figure 6C-8. Comparison with Figure 6C-1 confirms that the predominant mode in the aperture field is the $\mathbf{TM}_{11}$ mode, with two peaks in the E-plane cross-section.

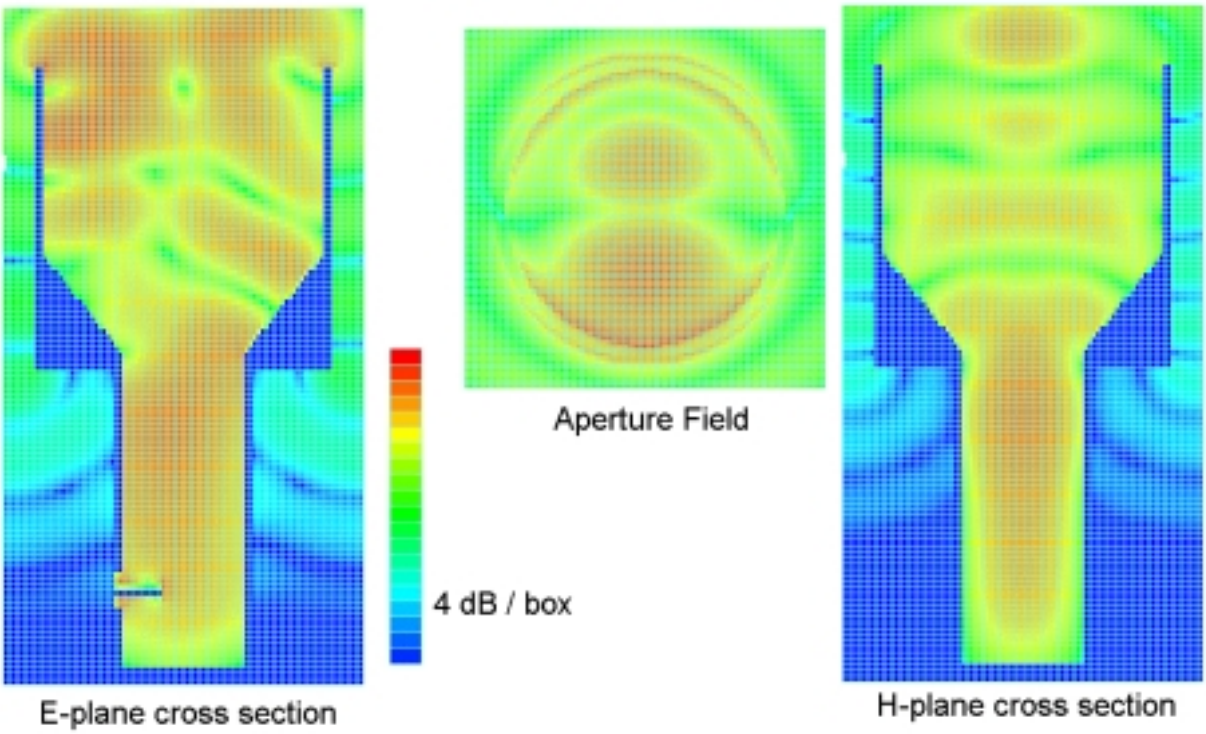

Figure 6C-8 Electric Fields in bad imitation of W2IMU dual-mode feedhorn by Zeland Fidelity

Other feeds use choke rings to reduce unwanted lobes. The VE4MA feed, with fields shown in Figure 6C-9, and the Chaparral-type feeds, with fields shown in Figure 6C-10, both have fields in the aperture of the central circular waveguide similar to the plain open waveguide, with high field intensity on the rim at top and bottom. The choke rings reduce the field traveling back along the guide walls and so reduce radiation to the side and rear. The multiple choke rings of the Chaparral-type feed are effective over a wider bandwidth than the single-ring of the VE4MA feed, but wide bandwidth is rarely important in amateur applications.

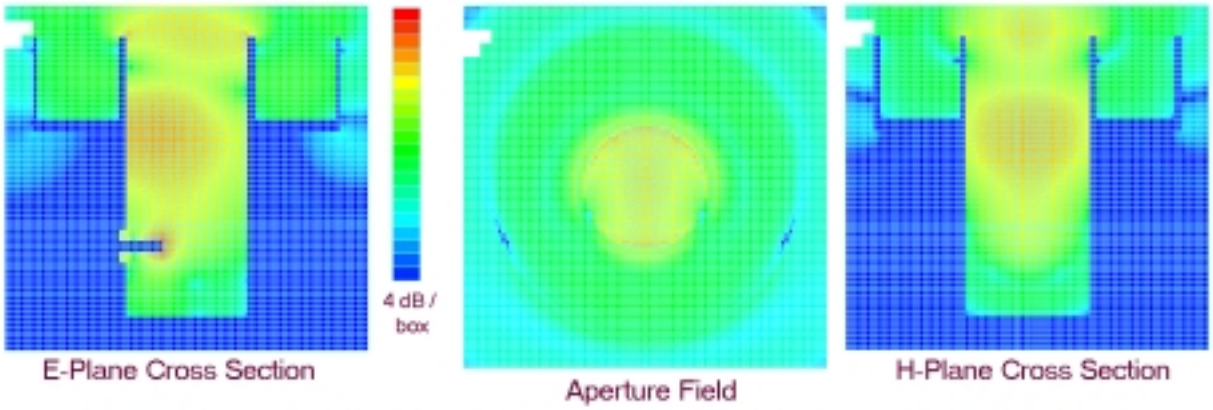

Figure 6C-9 Electric Fields in VE4MA feedhorn
by Zeland Fidelity

The left-hand diagram for the VE4MA feed shows an asymmetry in the field arriving at the aperture – an example of the effect of a short waveguide. One way to look at the problem, if the higher-order mode explanation doesn't help, is that the probe is closer to one wall than the other, so energy arrives first at the rim wall nearer the probe. When the guide is longer, the difference in length becomes less significant. Is this a real problem? Calculations on very short feeds often show a few degrees of squint in the radiation pattern, but since the illumination angle for these feeds is >100 degrees, the effect is probably not significant.

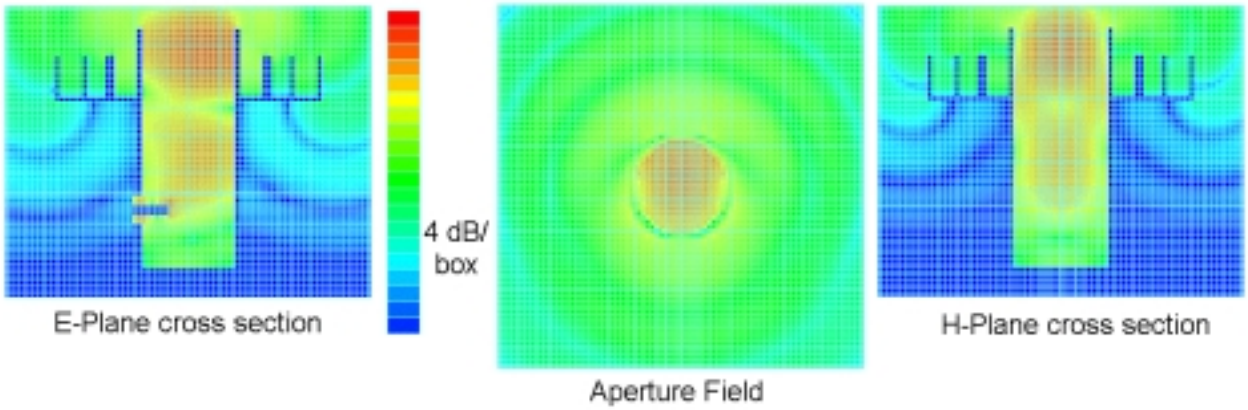

Figure 6C-10 Electric Fields in Chaparral-style feedhorn
by Zeland Fidelity

Rectangular horns

Can we improve the sidelobe performance of a rectangular waveguide like the circular feeds? It should be possible to add choke rings, but the rectangular cross section is much harder to machine than circular rings. We would also find that the rectangular cross-section provides a pattern that is not axisymetric, as we saw in the radiation patterns for an open rectangular waveguide in Figure 6C-4.

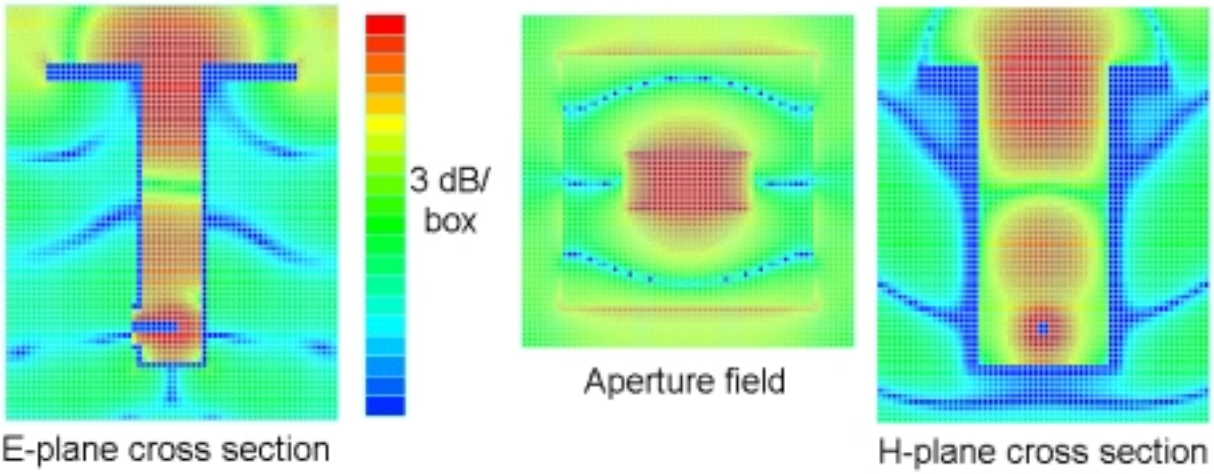

Figure 6C-11 Electric Fields in open WR-90 with flange
by Zeland Fidelity

What about a waveguide flange? The square flange is as ubiquitous as WR-90 waveguide, but I've never seen a radiation pattern published for an open waveguide with flange, so I had to try one. Figure 6C-11 shows the electric fields for an open WR-90 waveguide with a UG39/U square flange. The aperture field appears more circular. There is still significant field intensity at the top and bottom edges of the flange, but the field intensity back along the outside of the waveguide is reduced. The end result is a significant improvement in the far-field radiation patterns, particularly the front-to-back ratio. The calculated efficiency, as shown in Figure 6C-12, is significantly better than the plain open-ended waveguide in Figure 6C-4. This may be one of the better feeds available for a very deep dish with ***f*/D** around 0.25 to 0.3; it is certainly easy to find.

WR90 open with square flange at 10.368 GHz

Figure 6C-12 by Zeland Fidelity

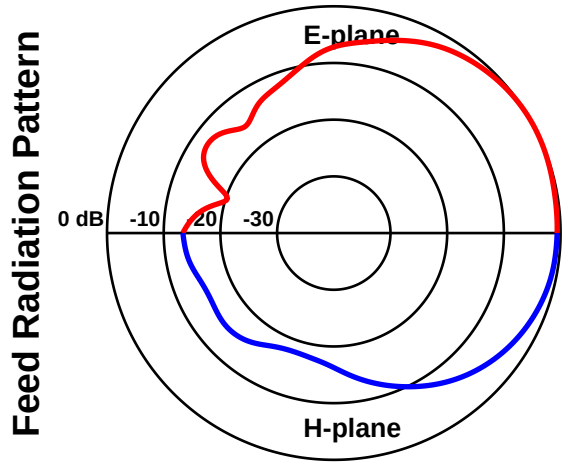

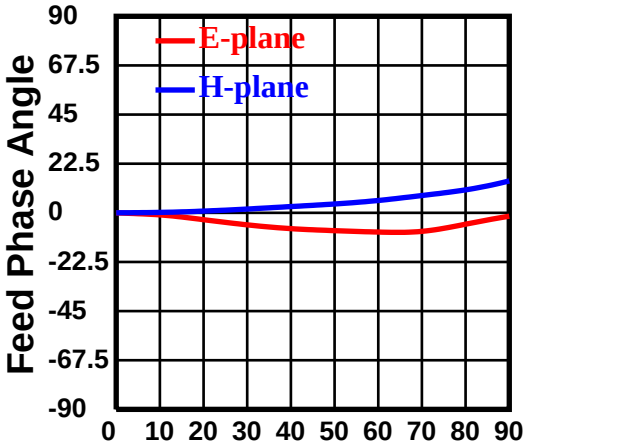

Dish diameter = 10 λ Feed diameter = 1 λ

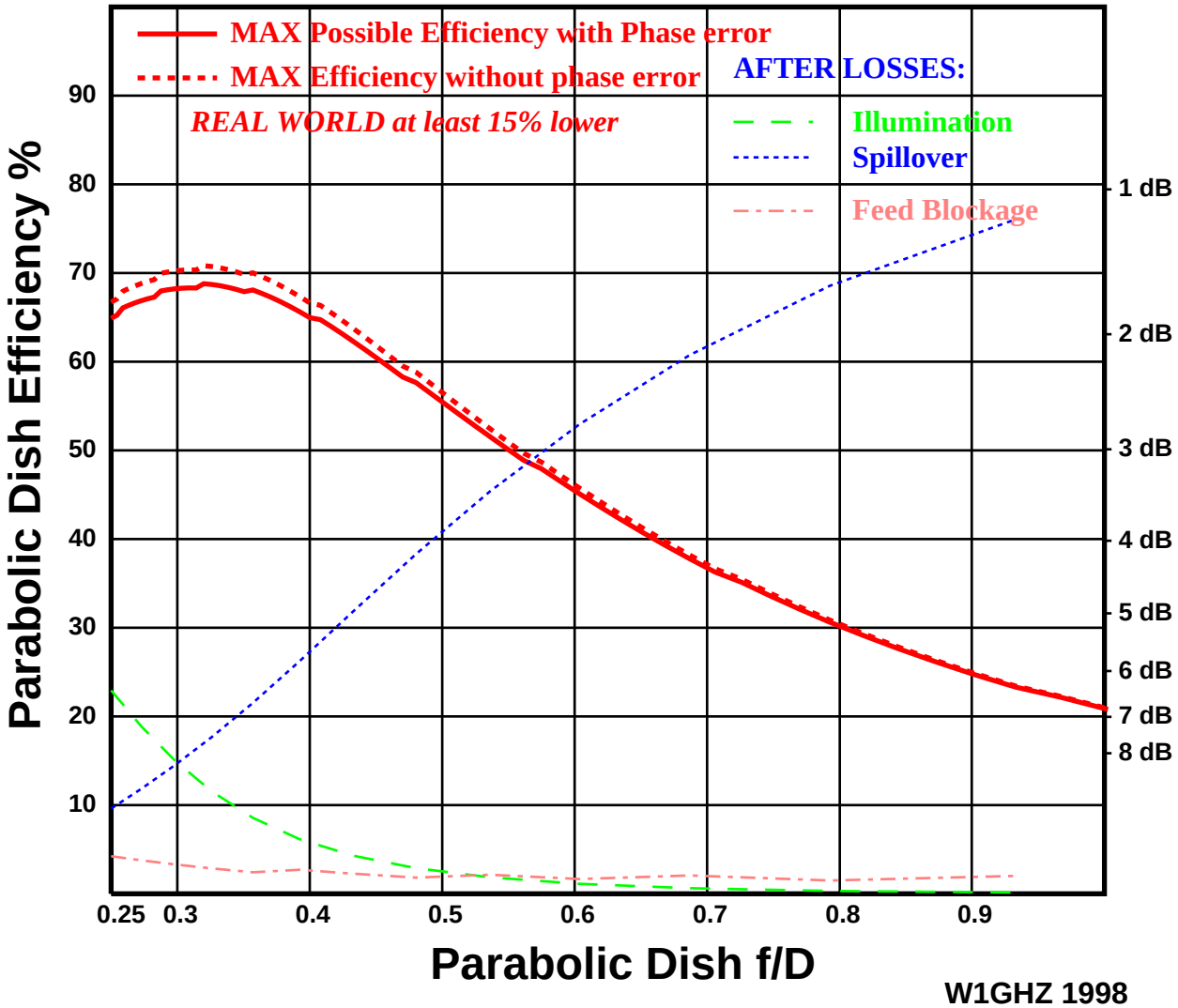

W1GHZ 1998

For a shallow dish with larger ***f*/D**, a rectangular horn can be a good feed. Figure 6C-13 shows the electric field in the 10 GHz rectangular feedhorn for a DSS offset dish described in section 6.4. The field spreads out radially from the throat of the horn along the flare so that it is approaching a spherical wavefront as it reaches the aperture. Thus, the phase center, or apparent source of the radiation, is inside the aperture — for large horns, the phase center is close to the throat.

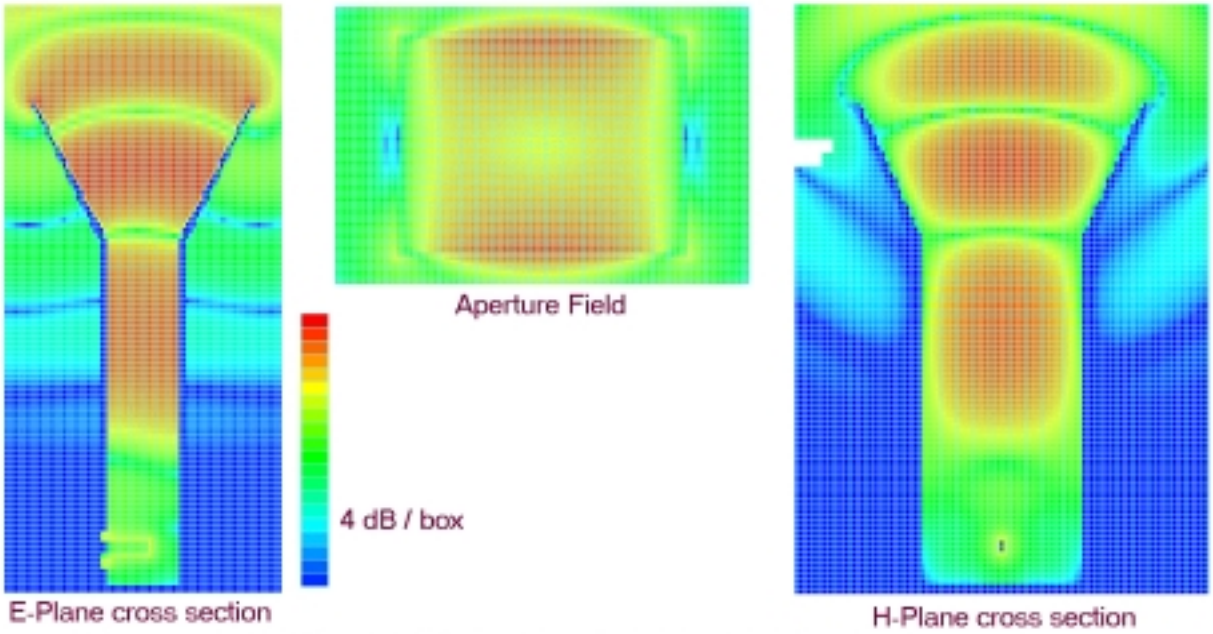

Figure 6C-13 Electric Fields in Rectangular horn feed for DSS dish
by Zeland Fidelity

Like the open-ended waveguide, there is high field intensity at the top and bottom rim of the aperture, resulting in the E-plane sidelobes seen in section 6.4. Still, the horn concentrates the majority of the radiated power in the main lobe. By adjusting the flare angle in the two planes separately, we may make the pattern more symmetric to provide an efficient feed.

Diagonal horns

A diagonal horn may be fed by a tapered transition from circular guide. We might expect the aperture field to be somewhat similar to the field in the circular guide, as sketched in section 6.5. The calculated fields for a diagonal horn 0.73λ square with no flare, in Figure 6C-14, show no sign of the constricted waist we saw in the circular guide; rather, the field has filled out toward all four corners, with higher field intensity at the top and bottom corners. The result is a radiation pattern with good symmetry in the E- and H-planes, shown in Figure 6C-15, and good calculated dish efficiency. Sidelobe level is somewhat higher in the E-plane due to the high field in the corners. The 45° planes do not match the principal planes, since neither the aperture nor the fields are really axisymmetric, so the pattern is not either. These results are comparable to the **NEC2** calculations for a slightly smaller diagonal horn, in section 6.5. The straight diagonal horn offers no real improvement on an open circular waveguide, so the extra metalwork does not seem worthwhile.

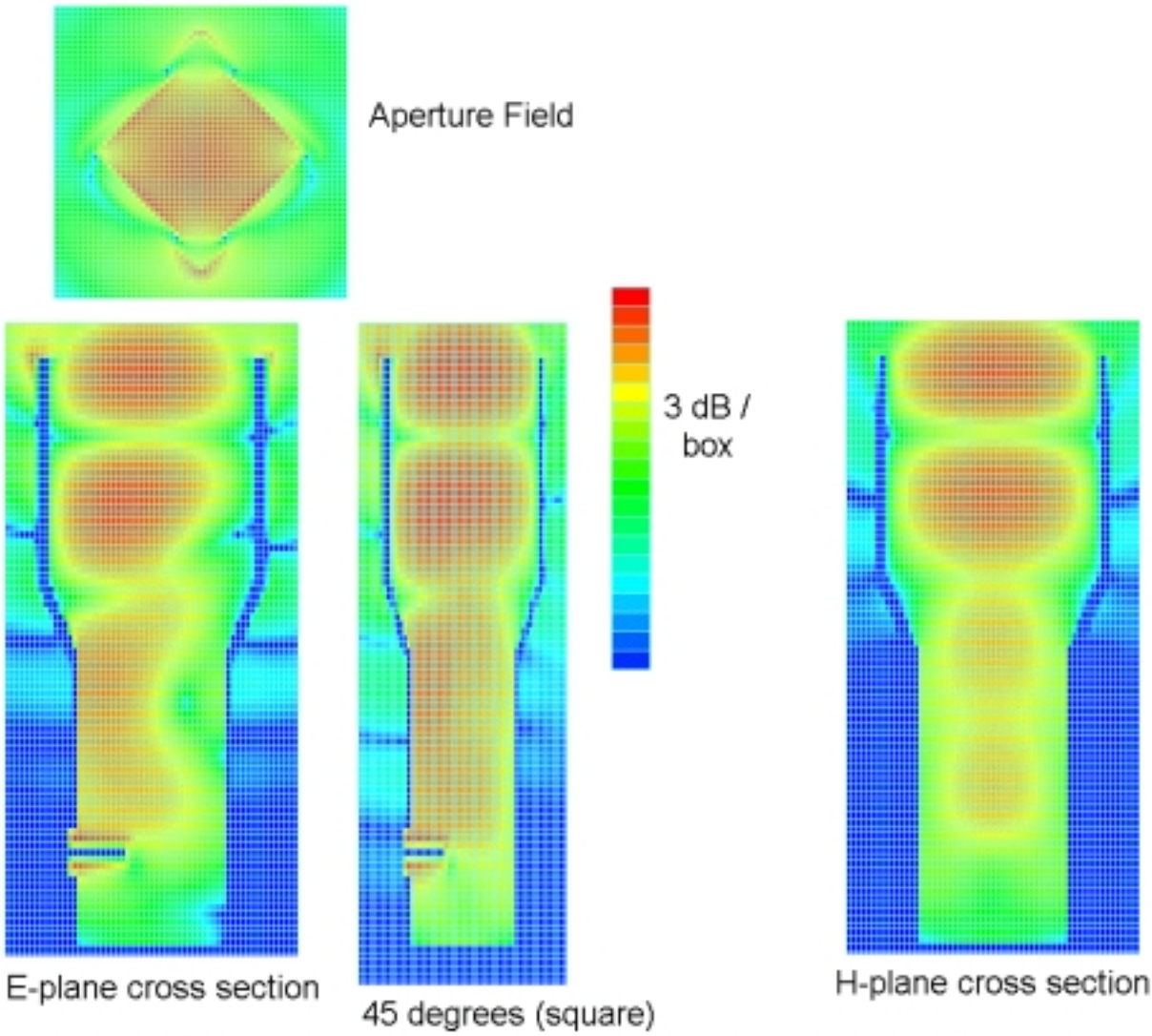

Figure 6C-14 Electric Fields in Diagonal horn feed with no flare
by Zeland Fidelity

Diagonal horn 0.73λ square, no flare, by Zeland Fidelity™

Figure 6C-15

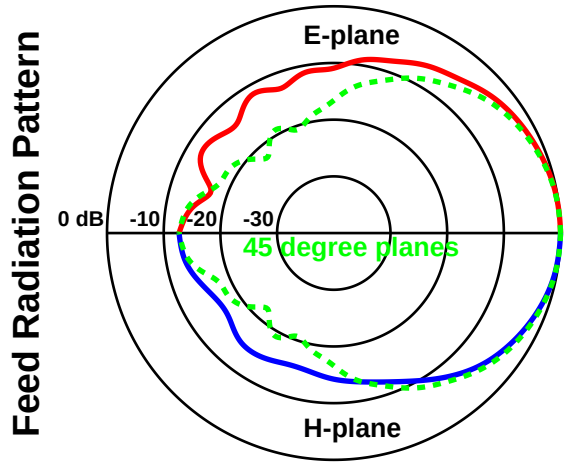

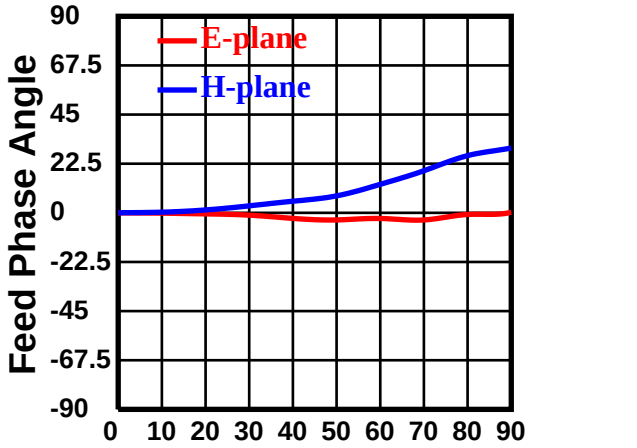

Dish diameter = 10 λ Feed diameter = 1 λ

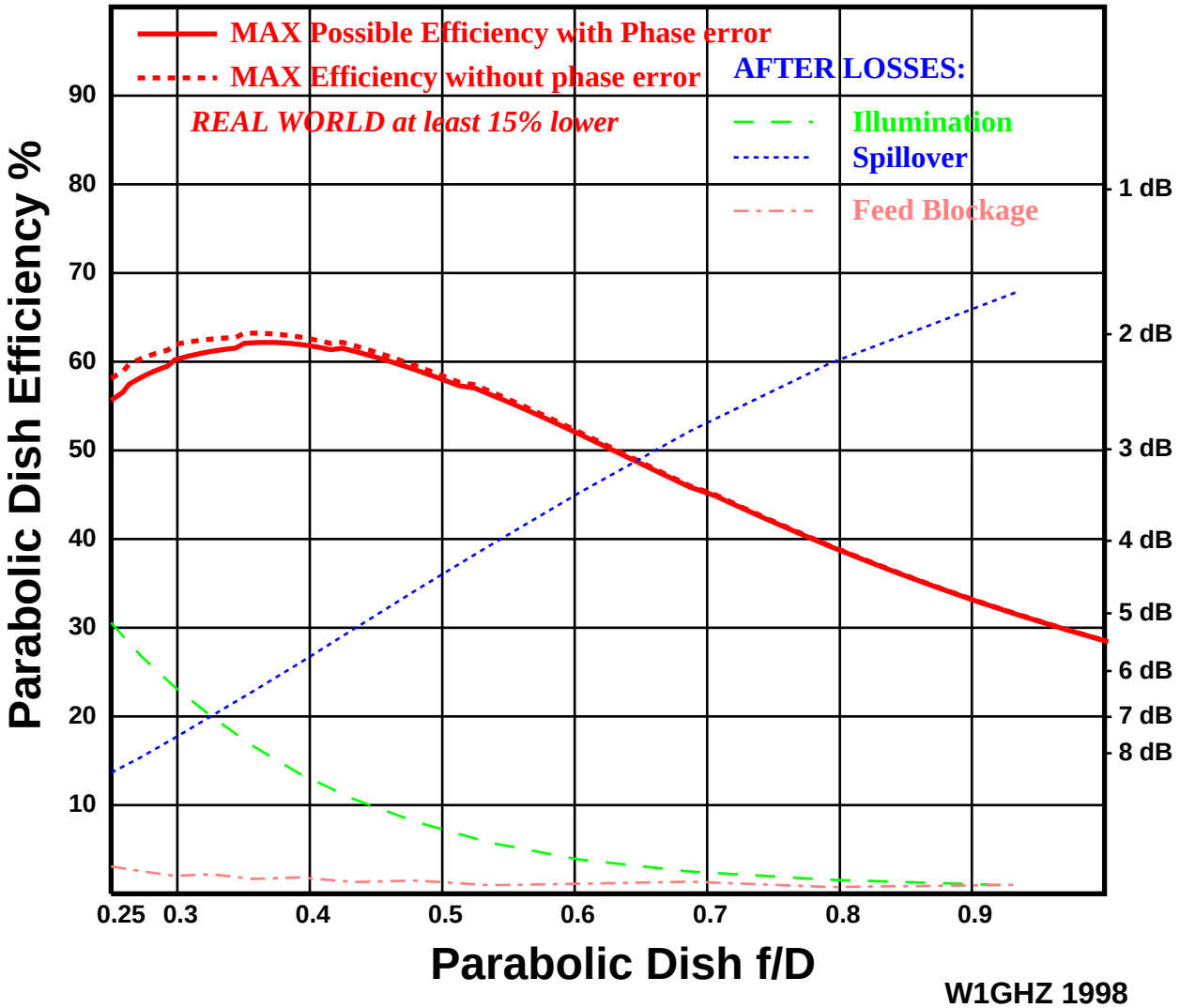

W1GHZ 1998

A diagonal horn with a gentle 14° flare to an aperture 1.4λ square, designed to feed an offset dish, has calculated fields shown in Figure 6C-16. The aperture field is slightly more uniform than the unflared horn, with a hint of a circular shape. The resulting far-field radiation patterns, shown in Figure 6C-17, have a good front-to-back ratio and low sidelobes in the E- and H-planes but somewhat higher levels in the 45-degree planes. Calculated efficiency is very similar to that calculated using Physical Optics in section 6-5 for the same dimensions.

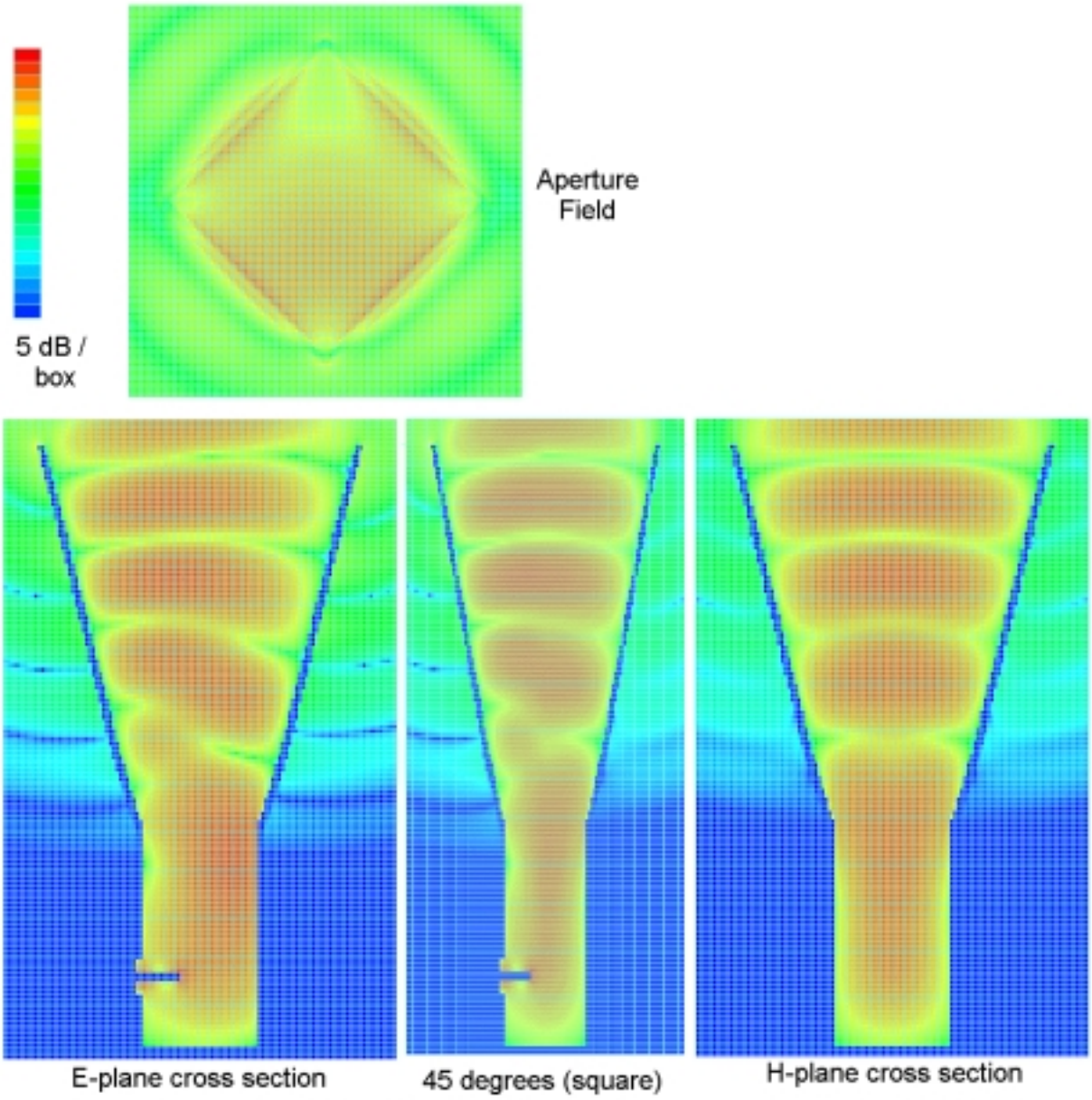

Figure 6C-16 Electric Fields in Diagonal horn feed with 14 degree flare
by Zeland Fidelity

10 GHz diagonal feedhorn, 1.4λ square, 14° flare,

by Zeland Fidelity™

Figure 6C-14

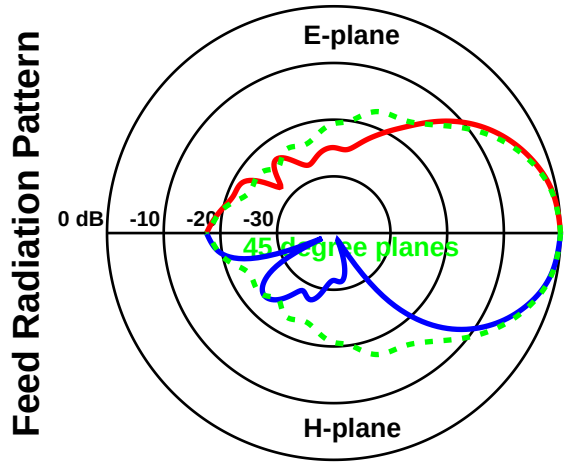

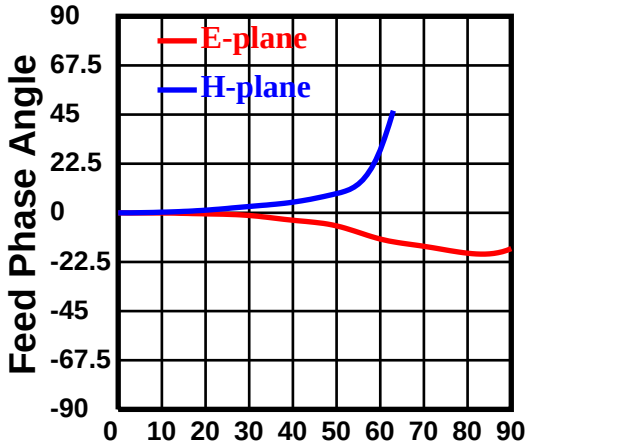

Dish diameter = 14 λ Feed diameter = 1.4 λ

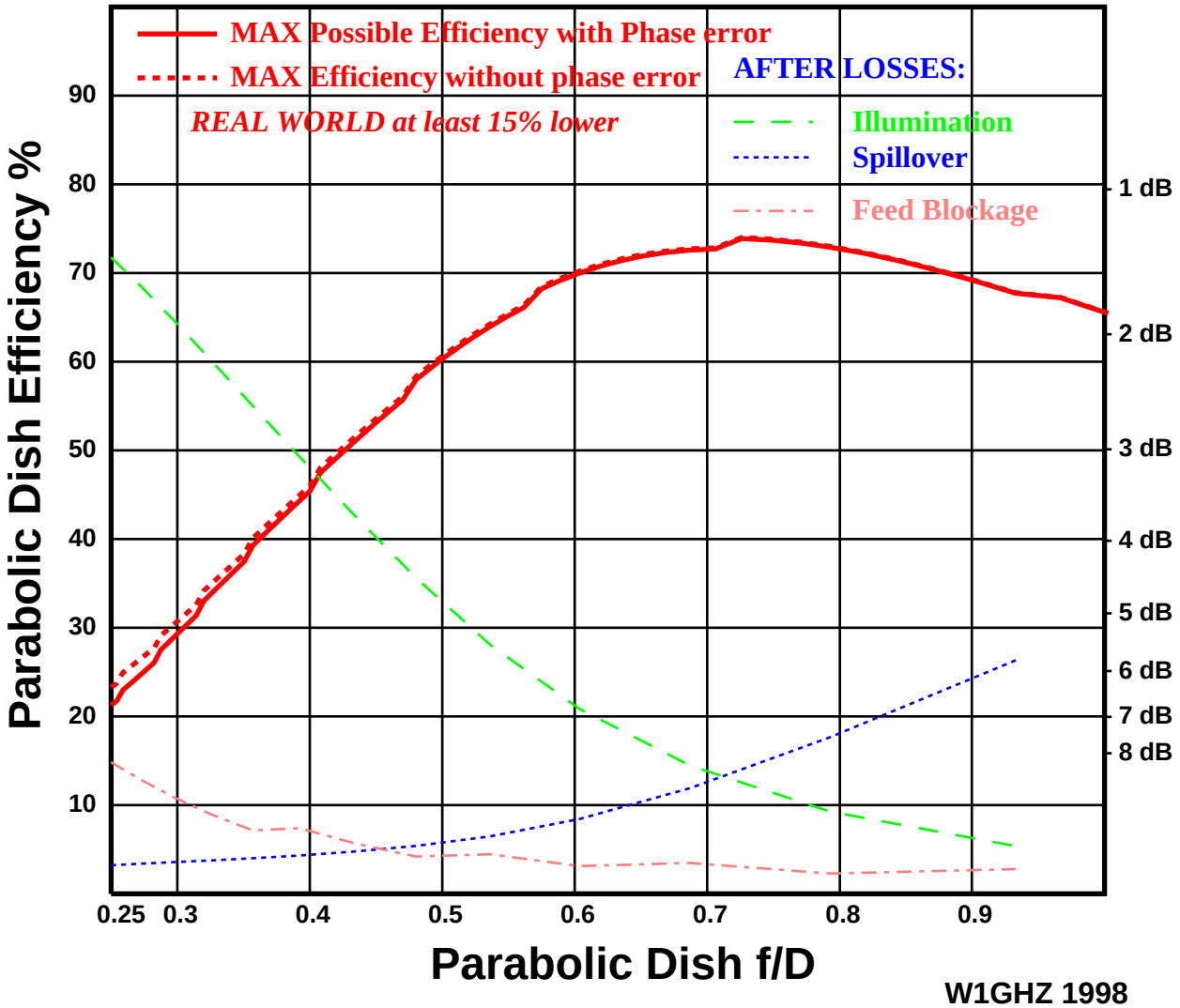

W1GHZ 1998

Penny feed

For a final example, we examine the electric field of a G4ALN “Penny” feed in Figure 6C-18. The field becomes bifurcated to radiate out the two slots on opposite sides of the waveguide, so that radiation must emanate from two distinct sources, like Figure 1-2e; interference and sidelobes are inevitable. The result is that aperture field has poor axial symmetry, like the resultant radiation patterns in section 6.7. The E-plane cross-section clearly shows diffraction of the field around the edges of the disk, resulting in the poor front-to-back ratio evident in section 6.7. The combination of high sidelobes and poor front-to-back ratio reduces the useful radiation reaching the reflector, so that dish efficiency with this feed is poor.

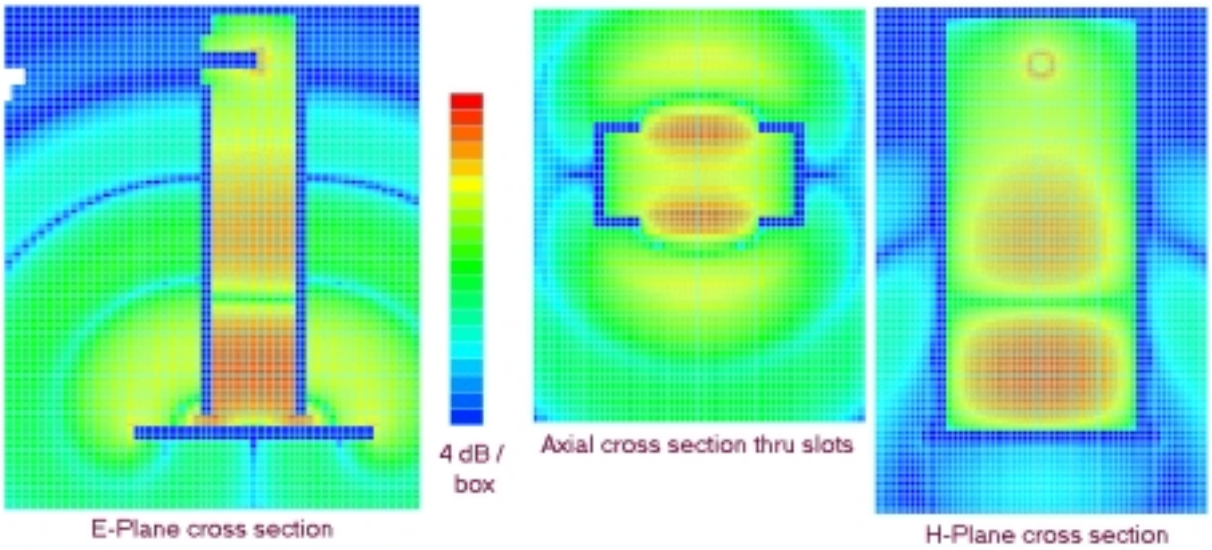

Figure 6C-18 Electric Fields in G4ALN Penny feed
by Zeland Fidelity

Summary

We have examined the calculated electric fields in and around some popular feed antennas to better understand the operation of these antennas. These examples illustrate different features found in the near field, so that we might better interpret near-field plots of other feeds. The goal is to help us develop a better intuition for antenna operation.

References

1. Zeland Software, Inc. http://www.zeland.com

2. Southworth, George C., *Principles and Applications of Waveguide Transmission*, van Nostrand, 1950.

3. E.V. Jull, *Aperture Antennas and Diffraction Theory*, Peter Peregrinus Ltd., 1981.

4. R.W.P. King, H.R. Mimno, & A.H. Wing, *Transmission Lines, Antennas, and Wave Guides*, McGraw-Hill, 1945, pp. 254-263.

5. "Fourier Waveform Analysis," *Reverence Data for Radio Engineers*, Sixth Edition, Howard W. Sams, 1975, Chapter 44.

6. J. Harrison, W5ZN, "W5ZN Dual Band 10 GHz / 24 GHz Feedhorn," *Proceedings of Microwave Update '98*, ARRL, 1998, pp. 189-190.

7. R.H. Turrin, (W2IMU), "Dual Mode Small-Aperture Antennas," *IEEE Transactions on Antennas and Propagation*, AP-15, March 1967, pp. 307-308. (reprinted in A.W. Love, *Electromagnetic Horn Antennas*, IEEE, 1976, pp. 214-215.)